

Unified Approach to Solve a Class of Strip and Microstrip-Like Transmission Lines

BHARATHI BHAT AND SHIBAN K. KOUL, STUDENT MEMBER, IEEE

Abstract — This paper presents a unified analytical approach to solve a class of shielded strip and shielded microstrip-like transmission lines with multilayer dielectrics under TEM-wave approximation. The analysis makes use of the variational technique in the space domain combined with the “transverse transmission line” method. Expressions are derived for the capacitance of a single line, coupled two-line and coupled four-line structures. The same formulas can be used for a class of such structures by the substitution of a single parameter, namely, the admittance at the charge plane, which can be obtained using the standard transmission line formulas. Numerical results of two special structures, namely, the broadside-coupled suspended microstrip lines, and broadside-coupled inverted microstrip lines, using two suspended, dielectric substrates are included. The technique presented is the simplest compared to any other analytical procedures reported in the literature.

I. INTRODUCTION

HERE EXISTS extensive literature dealing with the analytical and numerical solutions of strip and microstrip-like transmission lines. Both hybrid mode and quasi-static analyses have been reported. Of these, the hybrid mode approach is complicated but rigorous, while the quasi-static approach is much simpler but has a limited range of validity. However, the latter is known to give quite accurate results of characteristic impedance and guide wavelength, adequate for most MIC applications.

Several methods based on the TEM and quasi-TEM approximations have been reported. These include the conformal transformation method [1]–[4], the finite difference method [5]–[7], the integral equation method [8]–[10], and the variational method [11]–[14].

For the analysis of strip and microstrip-like transmission lines having two or more dielectric interfaces, the variational method is found to be the simplest. This method requires setting up of either the potential function or the Green's function for a particular configuration. These functions are generally derived by solving a set of algebraic equations obtained by applying the boundary conditions at various boundaries and interfaces [15]–[18]. For inhomogeneous structures, even this method becomes increasingly complicated with an increase in the number of dielectric layers. Recently Koul and Bhat [19]–[20] have presented an

analysis of microstrip-like transmission lines using the variational method in which the potential function and Green's function are derived using the “transverse transmission line” method [21].

The purpose of this paper is to present an unified approach to solve a class of stripline and microstrip-like transmission structures. The method is applicable to single as well as coupled lines in either the open or shielded configurations. Numerical results of some of the typical structures are compared with those reported in the literature using other techniques. In addition, computed results of characteristic impedance and phase velocity are presented for two new structures, namely, the broadside-coupled inverted microstrip lines and broadside-coupled suspended microstrip lines, using two suspended, dielectric substrates.

II. SINGLE-LINE STRUCTURES

In order to illustrate the simplicity of approach involved in the “transverse transmission line” method, we consider a shielded stripline as shown in structure A1 of Table I. The Green's function $G(x, y/x_0, y_0)$ due to a unit charge located at (x_0, y_0) satisfies the Poisson's differential equation

$$\nabla^2 G(x, y/x_0, y_0) = (-1/\epsilon) \delta(x - x_0) \delta(y - y_0) \quad (1)$$

where $\delta(x - x_0)$ and $\delta(y - y_0)$ are Dirac's delta functions and ϵ is the dielectric constant of the region containing the charge. In this problem, the Green's function can be expressed as

$$G(x, y/x_0, y_0) = \sum_n \sin(\beta_n x) G_n(y), \quad \beta_n = n\pi/c. \quad (2)$$

Substituting (2) into (1), $G_n(y)$ satisfies the following equation:

$$(d^2/dy^2 - \beta_n^2) G_n(y) = -(2/c\epsilon) \sin(\beta_n x_0) \delta(y - y_0). \quad (3)$$

$G_n(y)$ is now obtained using the “transverse transmission line” method. For a transmission line extending along the y -direction with a current source of intensity I_s located at $y = y_0$, the voltage V along the line satisfies the following

Manuscript received August 19, 1981; revised December 4, 1981.

The authors are with the Centre for Applied Research in Electronics, Indian Institute of Technology, Delhi, Hauz Khas, New Delhi 110016, India.

TABLE I

| STRUCTURE | ADMITTANCE Y AT $y = y_0$ |
|---|---|
| A1. SYMMETRIC STRIPLINE | |
| | |
| B1. SYMMETRIC EDGE COUPLED STRIPLINE | $2\epsilon_0\epsilon_r \coth(\frac{n\pi b}{2c})$ |
| | $2\epsilon_0\epsilon_r \coth(\frac{n\pi b}{2c})$ |
| A2. BROADSIDE OFFSET STRIPLINE | |
| | |
| B2. BROADSIDE OFFSET EDGE COUPLED STRIPLINE | $\epsilon_a \left[\epsilon_r \coth(\frac{n\pi}{c}(b-d)) + \epsilon_{r2} \left(\frac{\epsilon_{r3} \coth(\frac{n\pi b}{2c}) \coth(\frac{n\pi d}{c}) + \epsilon_{r2}}{\epsilon_{r2} \coth(\frac{n\pi d}{c}) + \epsilon_{r3} \coth(\frac{n\pi b}{2c})} \right) \right]$ |
| A3. MICROSTRIP | |
| | $\epsilon_0 \left[\coth(\frac{n\pi h}{c}) + \epsilon_r \coth(\frac{n\pi b}{c}) \right]$ |
| B3. EDGE COUPLED MICROSTRIP | |
| | $\epsilon_0 \left[\coth(\frac{n\pi h}{c}) + \epsilon_{r2} \left(\frac{\epsilon_{r1} \coth(\frac{n\pi b}{c}) \coth(\frac{n\pi a}{c}) + \epsilon_{r2}}{\epsilon_{r2} \coth(\frac{n\pi a}{c}) + \epsilon_{r1} \coth(\frac{n\pi b}{c})} \right) \right]$ |
| A4. DOUBLE LAYER MICROSTRIP | |
| | |
| B4. DOUBLE LAYER EDGE COUPLED MICROSTRIP | |
| | $\epsilon_0 \left[\coth(\frac{n\pi h}{c}) + \epsilon_{r2} \left(\frac{\epsilon_{r1} \coth(\frac{n\pi b}{c}) \coth(\frac{n\pi a}{c}) + \epsilon_{r2}}{\epsilon_{r2} \coth(\frac{n\pi a}{c}) + \epsilon_{r1} \coth(\frac{n\pi b}{c})} \right) \right]$ |
| A5. SANDWICHED MICROSTRIP | |
| | $\epsilon_0 \left[\epsilon_{r2} \left(\frac{\coth(\frac{n\pi h}{c}) \coth(\frac{n\pi a}{c}) + \epsilon_{r2}}{\epsilon_{r2} \coth(\frac{n\pi a}{c}) + \coth(\frac{n\pi h}{c})} \right) + \epsilon_{r1} \left(\frac{\coth(\frac{n\pi b}{c}) \coth(\frac{n\pi a}{c}) + \epsilon_{r1}}{\epsilon_{r1} \coth(\frac{n\pi a}{c}) + \coth(\frac{n\pi b}{c})} \right) \right]$ |
| B5. SANDWICHED EDGE COUPLED MICROSTRIP | |
| | $\epsilon_0 \left[\epsilon_{r2} \left(\frac{\coth(\frac{n\pi h}{c}) \coth(\frac{n\pi a}{c}) + \epsilon_{r2}}{\epsilon_{r2} \coth(\frac{n\pi a}{c}) + \coth(\frac{n\pi h}{c})} \right) + \epsilon_{r1} \left(\frac{\coth(\frac{n\pi b}{c}) \coth(\frac{n\pi a}{c}) + \epsilon_{r1}}{\epsilon_{r1} \coth(\frac{n\pi a}{c}) + \coth(\frac{n\pi b}{c})} \right) \right]$ |

MICROSTRIP WITH OVERLAY : $b = 0$
 INVERTED MICROSTRIP : $a_1 = 0, a_2 = a, \epsilon_{r2} = \epsilon_r$
 SUSPENDED MICROSTRIP : $a_2 = 0, a_1 = a, \epsilon_{r1} = \epsilon_r$

differential equation:

$$(d^2/dy^2 - \gamma^2)V = -(\gamma/Y_c)I_s \delta(y - y_0) \quad (4)$$

where γ is the propagation constant and Y_c is the characteristic admittance of the line. Setting $Y_c = \epsilon$ and comparing (3) and (4), we obtain

$$V \equiv G_n(y) \quad \gamma \equiv \beta_n \quad I_s \equiv (2/\beta_n c) \sin(\beta_n x_0). \quad (5)$$

Since the voltage on the transmission line at $y = y_0$ is given by $V = I_s/Y$, we have

$$G_n(y) = (2/\beta_n c Y) \sin(\beta_n x_0) \quad (6)$$

where Y is the admittance at the charge plane, $y = y_0$. Using the standard expression for the admittance of a section of transmission line, Y at the charge plane is obtained as the sum of admittances Y_1 and Y_2 , looking in

the positive and negative y -directions, respectively (see Table I). Substituting (6) into (2), the Green's function at the charge plane $y = y_0$, is expressed as

$$G(x, y_0/x_0, y_0) = \sum_{n=1}^{\infty} (2/n\pi Y) \sin(\beta_n x) \sin(\beta_n x_0), \quad (7)$$

The capacitance of the structure is obtained by using (7) in the following variational expression [22]:

$$C = \frac{\left[\int_{S_1} f(x) dx \right]^2}{\int_{S_1} \int_{S_1} G(x, y_0/x_0, y_0) f(x) f(x_0) dx dx_0} \quad (8)$$

where $f(x)$ is the charge distribution on the strip conductor

S_1 and can be assumed to be of the form

$$\begin{aligned} f(x) &= (1/w) \left[1 + A \left| (2/w)(x - c/2) \right|^3 \right], \\ &\quad (c-w)/2 \leq x \leq (c+w)/2 \\ &= 0, \quad \text{otherwise} \end{aligned} \quad (9)$$

where A is an arbitrary constant and is determined by maximizing the line capacitance C . Substituting (7) and (9) in (8) and evaluating the integral, we obtain

$$C = \frac{(1+0.25A)^2}{\sum_{n \text{ odd}} (T_n P_n / Y)} \quad (10)$$

where

$$T_n = (L_n + A M_n)^2 \quad (11a)$$

$$L_n = \sin(\beta_n w/2) \quad (11b)$$

$$\begin{aligned} M_n &= (2/\beta_n w)^3 \left[3 \left\{ (\beta_n w/2)^2 - 2 \right\} \cos(\beta_n w/2) \right. \\ &\quad \left. + (\beta_n w/2) \left\{ (\beta_n w/2)^2 - 6 \right\} \sin(\beta_n w/2) + 6 \right] \end{aligned} \quad (11c)$$

$$P_n = (2/n\pi)(2/\beta_n w)^2 \quad (11d)$$

$$A = - \frac{\sum_{n \text{ odd}} (L_n - 4M_n) L_n P_n / Y}{\sum_{n \text{ odd}} (L_n - 4M_n) M_n P_n / Y}. \quad (11e)$$

Expression (10) can be numerically solved to obtain the line capacitance. Combining (10) with standard formulas [22], the characteristic impedance and phase velocity can be calculated. The above expressions are quite general and can be used to obtain data for a class of stripline and microstrip structures with single strip conductor by simply substituting the appropriate expression for Y at the charge plane. Table I gives expressions for Y for some of the single-line structures.

III. TROUGH TRANSMISSION STRUCTURES

Structures A3–A5 in Table I reduce to the corresponding trough lines when the top wall is moved to infinity in the positive y -direction ($h = \infty$). The admittance Y at the charge plane for each trough line is obtained by setting $\coth(n\pi h/c) = 1$ in the corresponding expression given in Table I. For the same charge distribution as in (9), the capacitance of trough line is calculated from (10) and (11) by substituting the appropriate expression for Y .

IV. EDGE-COUPLED TWO CONDUCTOR SYMMETRIC STRUCTURES

Structures B1–B5 of Table I show some typical edge-coupled symmetric lines. Utilizing the symmetry with respect to the plane pp' at $x = c/2$ (as shown in structure B1), the even- and odd-mode capacitances can be obtained by placing a magnetic wall and an electric wall, respectively, at pp' and by considering half the structure between

$x = 0$ and $c/2$. The even- and odd-mode charge distributions are assumed to be of the form

$$\begin{aligned} f(x) \left(\begin{array}{c} \text{even} \\ \text{odd} \end{array} \right) &= (1/w) \\ &\quad \cdot \left[1 + A \left(\begin{array}{c} \text{even} \\ \text{odd} \end{array} \right) \left| (2/w)(x - (c-s-w)/2) \right|^3 \right], \\ &\quad ((c-s)/2) - w \leq x \leq (c-s)/2 \\ &= 0, \quad \text{otherwise.} \end{aligned} \quad (12)$$

Applying the “transverse transmission line” method, the even- and odd-mode Green’s functions can be expressed as

$$G(x, y_0/x_0, y_0) \left(\begin{array}{c} \text{even} \\ \text{odd} \end{array} \right) = \sum_{n \left(\begin{array}{c} \text{odd} \\ \text{even} \end{array} \right)} (4/n\pi Y) \sin(\beta_n x_0) \sin(\beta_n x) \quad (13)$$

where

$$\beta_n = n\pi/c. \quad (13)$$

The expression for the admittance Y at the charge plane $y = y_0$ for each coupled line structure is the same as that for the corresponding single conductor configuration (see Table I). It may be noted that the expression for Y is the same for both even- and odd-mode excitations.

The variational expression for the capacitance C is given by

$$C \left(\begin{array}{c} \text{even} \\ \text{odd} \end{array} \right) = \frac{(1+0.25 A \left(\begin{array}{c} \text{even} \\ \text{odd} \end{array} \right))^2}{\sum_{n \left(\begin{array}{c} \text{odd} \\ \text{even} \end{array} \right)} (T_n P_n / Y)} \quad (14)$$

where

$$T_n = (L_n + M_n A \left(\begin{array}{c} \text{even} \\ \text{odd} \end{array} \right))^2 \quad (15a)$$

$$L_n = \sin(\beta_n w/2) \sin(\beta_n (c-s-w)/2) \quad (15b)$$

$$\begin{aligned} M_n &= (2/\beta_n w)^3 \sin(\beta_n (c-s-w)/2) \\ &\quad \cdot \left[3 \left\{ (\beta_n w/2)^2 - 2 \right\} \cos(\beta_n w/2) \right. \\ &\quad \left. + (\beta_n w/2) \left\{ (\beta_n w/2)^2 - 6 \right\} \sin(\beta_n w/2) + 6 \right] \end{aligned} \quad (15c)$$

$$A \left(\begin{array}{c} \text{even} \\ \text{odd} \end{array} \right) = - \frac{\sum_{n \left(\begin{array}{c} \text{odd} \\ \text{even} \end{array} \right)} (L_n - 4M_n) L_n P_n / Y}{\sum_{n \left(\begin{array}{c} \text{odd} \\ \text{even} \end{array} \right)} (L_n - 4M_n) M_n P_n / Y} \quad (15d)$$

$$P_n = (4/n\pi)(2/\beta_n w)^2. \quad (15e)$$

V. SINGLE CONDUCTOR EDGE OFFSET STRUCTURES

In each of the structures, A1–A5, of Table I, if the strip conductor at $y = y_0$ is displaced asymmetrically about $x = c/2$, the corresponding edge-offset structure results. Fig. 1 shows a typical edge-offset stripline with spacing s between the right wall and the nearest edge of the strip conductor. The capacitance of edge-offset line is the same as the odd-mode capacitance of one strip with respect to ground

TABLE II

| STRUCTURE | ADMITTANCE Y AT $y = y_0$ |
|---|---|
| A1. HOMOGENEOUS BROADSIDE COUPLED STRIPLINE | $A1-A5 \begin{cases} p=1 & \text{even mode} \\ p=-1 & \text{odd mode} \end{cases}$ |
| B1 BROADSIDE-EDGE COUPLED STRIPLINES | $B1-B5 \begin{cases} p=1 & \begin{cases} \text{even even mode} \\ \text{odd even mode} \end{cases} \\ p=-1 & \begin{cases} \text{even odd mode} \\ \text{odd odd mode} \end{cases} \end{cases}$ |
| A2. BROADSIDE COUPLED MICROSTRIP LINES | $\epsilon_0 \epsilon_r [\coth(\frac{n\pi}{2c}(b-d)) + \tanh(\frac{n\pi d}{2c})]^p$ |
| B2 BROADSIDE-EDGE COUPLED MICROSTRIP LINES | $\epsilon_0 [\epsilon_r \coth(\frac{n\pi}{2c}(b-d)) + \tanh(\frac{n\pi d}{2c})]^p$ |
| A3. BROADSIDE COUPLED MICROSTRIP LINES WITH INVERTED DIELECTRIC | $\epsilon_0 [\coth(\frac{n\pi}{2c}(b-d)) + \epsilon_r (\tanh(\frac{n\pi d}{2c})]^p$ |
| B3 BROADSIDE-EDGE COUPLED MICROSTRIP LINES WITH INVERTED DIELECTRIC | $\epsilon_0 [\coth(\frac{n\pi}{2c}(b-d)) + \epsilon_r (\tanh(\frac{n\pi d}{2c})]^p$ |
| A4 BROADSIDE COUPLED INVERTED MICROSTRIP LINES | $\epsilon_0 [\coth(\frac{n\pi}{2c}(b-d)) + \epsilon_r (\tanh(\frac{n\pi d}{2c})]^p$ |
| B4 BROADSIDE-EDGE COUPLED INVERTED MICROSTRIP LINES | $\epsilon_0 [\coth(\frac{n\pi}{2c}(b-d)) + \epsilon_r (\tanh(\frac{n\pi d}{2c})]^p$ |
| A5. BROADSIDE COUPLED SUSPENDED MICROSTRIP LINES | $\epsilon_0 [\coth(\frac{n\pi}{2c}(b-d)) + \epsilon_r (\tanh(\frac{n\pi d}{2c})]^p$ |
| B5 BROADSIDE-EDGE COUPLED SUSPENDED MICROSTRIP LINES | $\epsilon_0 [\coth(\frac{n\pi}{2c}(b-d)) + \epsilon_r (\tanh(\frac{n\pi d}{2c})]^p$ |

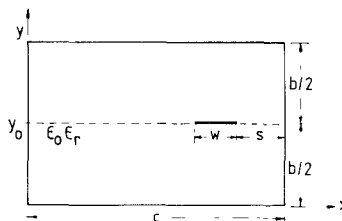


Fig. 1. Edge-offset stripline.

of a corresponding coupled line structure having the same dielectric media. Hence (14) and (15) for the odd-mode case can be directly used with c replaced by $2c$ and s replaced by $2s$.

VI. BROADSIDE-COUPLED SYMMETRIC STRUCTURES

Consider a typical broadside-coupled symmetric stripline as shown in structure A1 of Table II. Using the symmetry about $y = b/2$, the structure can be analyzed using the

even- and odd-mode method. For the even-mode excitation, the plane qq' at $y = b/2$ is replaced by a magnetic wall, while for the odd mode it is replaced by an electric wall. The problem thus reduces to that of finding the capacitance of half the structure between $y = 0$ and $b/2$ with the appropriate boundary wall at qq' . For the same charge distribution as given by (9), the capacitance can be calculated using (10) and (11) by substituting the appropriate expressions for Y for the even- and odd-mode excitations. Thus

$$C_{\text{odd}}^{\text{(even)}} = \frac{\left(1 + 0.25A_{\text{odd}}^{\text{(even)}}\right)^2}{\sum_{n \text{ odd}} \left(T_n P_n / Y_{\text{odd}}^{\text{(even)}}\right)} \quad (16a)$$

$$T_n = \left(L_n + M_n A_{\text{odd}}^{\text{(even)}} \right)^2 \quad (16b)$$

where L_n , M_n , and P_n are given by 11(b), 11(c), and 11(d),

respectively. Y_{even} and Y_{odd} refer to the even- and odd-mode admittances at the charge plane $y = y_0$ when only half the structure between $y = 0$ and $b/2$ is considered. A_{even} and A_{odd} are obtained from (11e) by replacing Y with Y_{even} and Y_{odd} , respectively. Expression (16) is applicable to any broadside-coupled, two conductor structure having symmetry with respect to the plane $y = b/2$. Table II gives expressions for the even- and odd-mode admittances for a class of such structures.

VII. COMBINED BROADSIDE AND EDGE-COUPLED SYMMETRIC FOUR-LINE STRUCTURES

Consider a typical four-line homogeneous stripline shown in structure B1 of Table II. Using the symmetry with respect to pp' and qq' , the structure can be analyzed in terms of the following four modes:

- 1) even-even mode pp' magnetic wall, qq' magnetic wall;
- 2) even-odd mode pp' magnetic wall, qq' electric wall;
- 3) odd-even mode pp' electric wall, qq' magnetic wall;
- 4) odd-odd mode pp' electric wall, qq' electric wall.

It now suffices to analyze one-quarter of the structure, lying between $0 \leq x \leq c/2$ and $0 \leq y \leq b/2$ with appropriate boundary conditions corresponding to the four modes.

For a charge distribution specified by (12), the Green's function is given by (13), with n odd for cases 1 and 2 and n even for cases 3 and 4. The admittance Y at $y = y_0$ obtained when qq' is a magnetic wall is denoted by Y_{even} (for cases 1 and 3) and that obtained when qq' is an electric wall is denoted by Y_{odd} (for cases 2 and 4). Thus, the capacitance expression (14) can be written as

$$C \begin{pmatrix} \text{even-even} \\ \text{even-odd} \\ \text{odd-even} \\ \text{odd-odd} \end{pmatrix} = \frac{\left(1 + 0.25 A \begin{pmatrix} \text{even-even} \\ \text{even-odd} \\ \text{odd-even} \\ \text{odd-odd} \end{pmatrix}\right)^2}{\sum_n \begin{pmatrix} \text{odd} \\ \text{odd} \\ \text{even} \\ \text{even} \end{pmatrix} \left(T_n P_n / Y \begin{pmatrix} \text{even} \\ \text{odd} \\ \text{even} \\ \text{odd} \end{pmatrix}\right)} \quad (17a)$$

$$T_n = \left(L_n + M_n A \begin{pmatrix} \text{even-even} \\ \text{even-odd} \\ \text{odd-even} \\ \text{odd-odd} \end{pmatrix}\right)^2 \quad (17b)$$

and

$$A \begin{pmatrix} \text{even-even} \\ \text{even-odd} \\ \text{odd-even} \\ \text{odd-odd} \end{pmatrix} = - \frac{\sum_n \begin{pmatrix} \text{odd} \\ \text{odd} \\ \text{even} \\ \text{even} \end{pmatrix} (L_n - 4M_n) L_n / Y \begin{pmatrix} \text{even} \\ \text{odd} \\ \text{even} \\ \text{odd} \end{pmatrix}}{\sum_n \begin{pmatrix} \text{odd} \\ \text{odd} \\ \text{even} \\ \text{even} \end{pmatrix} (L_n - 4M_n) M_n / Y \begin{pmatrix} \text{even} \\ \text{odd} \\ \text{even} \\ \text{odd} \end{pmatrix}} \quad (17c)$$

where L_n , M_n , and P_n are given by (15b), (15c), and (15e), respectively. Admittance expressions for various four-line structures, B1–B5, are the same as those for the corresponding two-line structures, A1–A5, shown in Table II;

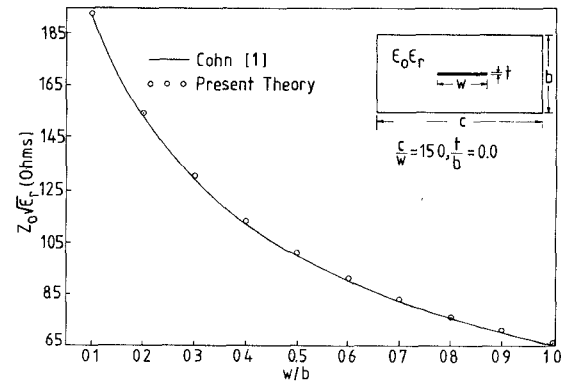


Fig. 2. Comparison of computed characteristic impedance of symmetric stripline with Cohn [1].

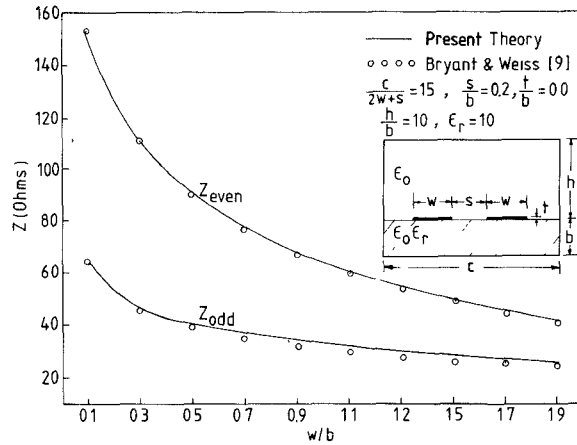


Fig. 3. Comparison of computed even- and odd-mode impedances of coupled microstrip lines with Bryant and Weiss [9].

where with $P = 1$, $Y = Y_{\text{even}}$ for "even-even" and "odd-even" modes and with $P = -1$, $Y = Y_{\text{odd}}$ for "even-odd" and "odd-odd" modes.

VIII. NUMERICAL RESULTS AND DISCUSSION

The computed impedance characteristics of some of the typical structures are compared with those reported in the literature using other methods for the same structural parameters. Fig. 2 shows comparison of impedance characteristics of a symmetrical stripline with that computed from the expressions given in Cohn [1]. The even- and odd-mode impedances of coupled microstrip lines are compared with those reported by Bryant and Weiss [9] in Fig. 3. The impedance characteristics computed for two types of broadside-coupled symmetric structures are compared with the results reported by Bahl and Bhartia [15] and Allen and Estes [18] in Figs. 4 and 5, respectively. In the cases considered in [1], [9], and [15], the structures have no side walls. In order to conform to this situation, in the present computations, the side walls are assumed sufficiently apart from the strip conductor so that they have negligible effect on the characteristic impedance. This is achieved by choosing $c/(2w+s) = 15$ for edge-coupled microstrip lines and $c/w = 15$ for the remaining structures. In all the cases, there is good agreement between the

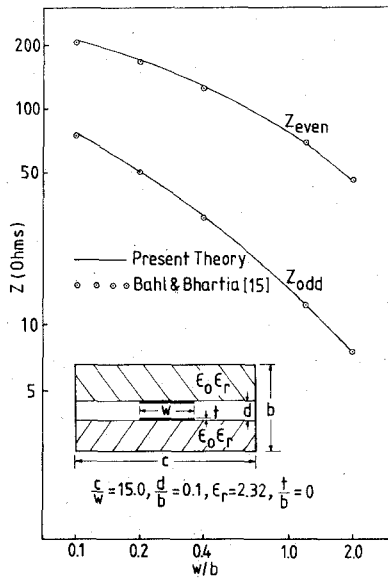


Fig. 4. Comparison of computed even- and odd-mode impedances of broadside-coupled microstrip lines with Bahl and Bhartia [15].

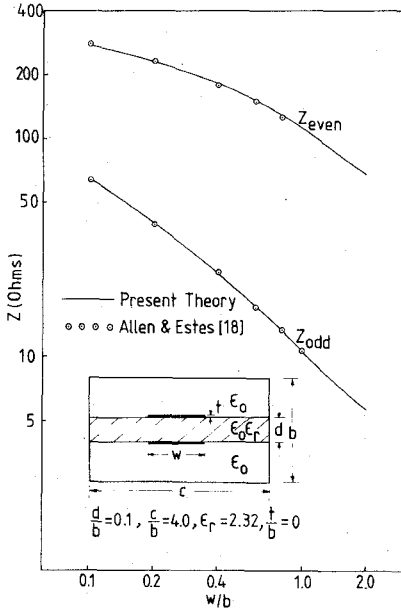


Fig. 5. Comparison of computed even- and odd-mode impedances of broadside-coupled microstrip lines with inverted dielectric with Allen and Estes [18].

present theoretical values and those reported by other authors.

Numerical computations of the even- and odd-mode impedances and phase velocities of a number of other structures given in Tables I and II have also been carried out. However, for want of adequate space, the results of only two new structures, namely, the broadside-coupled suspended microstrip and the broadside-coupled inverted microstrip, using two suspended dielectrics, are presented. For the broadside-coupled suspended microstrip, the variations of Z_{0e} and Z_{0o} as a function of w/b for $a/b = 0.1$ and $\epsilon_r = 2.32$, with d/b as a parameter are plotted in Fig.

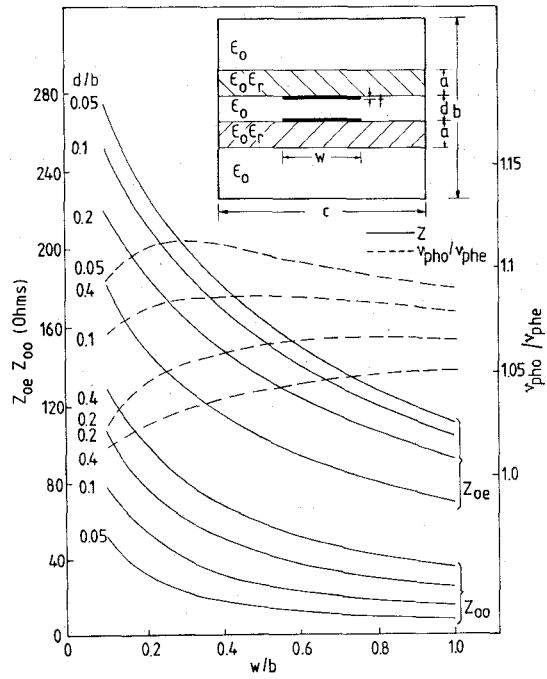


Fig. 6. Even- and odd-mode impedances and modal phase velocity ratio of broadside-coupled suspended microstrip lines: $a/b = 0.1$, $c/b = 4.0$, $t/b = 0$, $\epsilon_r = 2.32$.

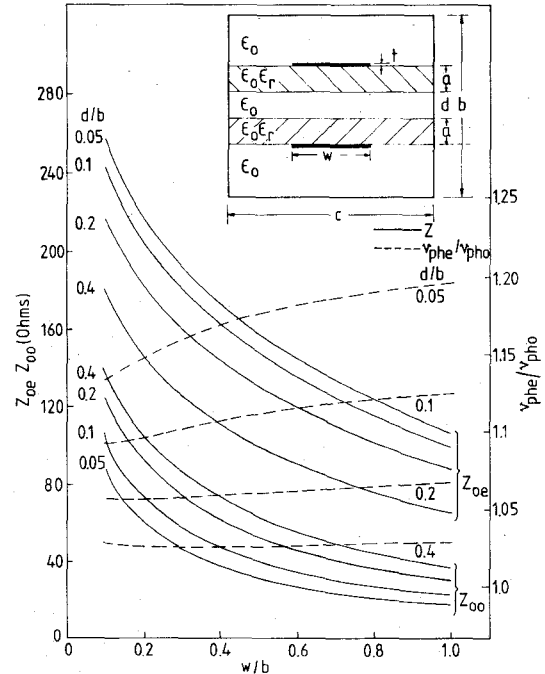


Fig. 7. Even- and odd-mode impedances and modal phase velocity ratio of broadside-coupled inverted microstrip lines: $a/b = 0.05$, $c/b = 4.0$, $t/b = 0$, $\epsilon_r = 2.32$.

6. Superimposed on these graphs are the variations of the modal phase velocity ratio $v_{\text{pho}}/v_{\text{phe}}$. As expected, with increase in the air gap d , Z_{0e} decreases. For odd-mode excitation, the broadside-coupled suspended microstrip is similar to the conventional, inverted microstrip for small values of d , and is similar to the suspended microstrip [19].

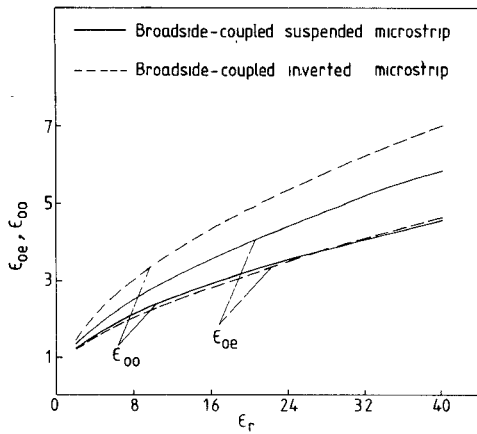


Fig. 8. Even- and odd-mode effective dielectric constant of broadside-coupled inverted microstrip lines, and broadside-coupled suspended microstrip lines, as a function of ϵ_r : $w/b = 0.1$, $a/b = d/b = 0.1$, $c/b = 4.0$, $t/b = 0$

for large values of d . Consequently, with increasing d , the odd-mode impedance increases initially and then decreases. For the structural parameters chosen, Z_{0e} and v_{phe}/v_{phe} decrease while Z_{0o} increases with an increase in d/b . For the broadside-coupled inverted microstrip, Fig. 7 shows the variations of Z_{0e} , Z_{0o} and v_{phe}/v_{phe} as a function of w/b for $a/b = 0.05$ and $\epsilon_r = 2.32$. The variations of Z_{0e} , Z_{0o} and v_{phe}/v_{phe} are similar to those of the broadside-coupled suspended microstrip lines. It is seen that both these structures are nearly homogeneous in the sense that they yield small deviations from equal modal phase velocities; typically less than 1.38 for most practical configurations. Compared with the conventional, broadside-coupled microstrip [15], the values of effective dielectric constants in the case of broadside-coupled suspended microstrip and broadside-coupled inverted microstrip considered here are much less (Fig. 8), permitting their use at millimeter-wave frequencies.

IX. CONCLUSION

The variational technique combined with the "transverse transmission line" method provides a simple unified approach to solve a class of stripline and microstrip-like transmission structures. In the case of coupled lines, any symmetric structure which can be resolved into even- and odd-mode configurations can be analyzed. Expressions are derived for the capacitance of a single line, coupled two-line, and coupled four-line structures. These expressions are general and can be used for a class of such structures by simply changing the admittance parameter Y at the charge plane $y = y_0$. Comparison of computed values of characteristic impedance for some of the typical structures show good agreement with those reported in the literature using other techniques. Numerical results of characteristic impedance and phase velocity are reported for two new structures, namely, the broadside-coupled suspended microstrip lines and the broadside-coupled inverted microstrip lines. These structures are nearly homogeneous in the

sense that they yield small deviations from equal modal phase velocities. Therefore, they can be used as high directivity backward wave couplers for realizing tight coupling at higher frequencies without using any dielectric overlay. The technique presented in this paper is the simplest compared to any other analytical procedures reported in the literature.

REFERENCES

- [1] S. B. Cohn, "Characteristic impedance of shielded-strip transmission line," *IRE Trans. Microwave Theory Tech.*, vol. MTT-2, pp. 52-55, July 1954.
- [2] M. V. Schneider, "Microstrip lines for microwave integrated circuits," *Bell Syst. Tech. J.*, vol. 48, pp. 1421-1444, May-June 1969.
- [3] H. A. Wheeler, "Transmission line properties of parallel strips separated by a dielectric sheet," *IEEE Trans. Microwave Theory Tech.*, vol. MTT-13, pp. 172-185, March 1965.
- [4] R. Pregla, "Calculation of the distributed capacitances and phase velocities in coupled microstrip lines by conformal mapping techniques," *Arch. Elek. Übertragung*, vol. 26, pp. 470-474, Oct. 1972.
- [5] H. E. Stinehelfer, "An accurate calculation of uniform microstrip transmission lines," *IEEE Trans. Microwave Theory Tech.*, vol. MTT-16, pp. 439-444, July 1968.
- [6] J. S. Hornsby and A. Gopinath, "Numerical analysis of a dielectric loaded waveguide with a microstrip line: Finite difference methods," *IEEE Trans. Microwave Theory Tech.*, vol. MTT-17, pp. 684-690, Sept. 1969.
- [7] H. E. Green, "The numerical solution of some important transmission line problems," *IEEE Trans. Microwave Theory Tech.*, vol. MTT-13, pp. 676-692, Sept. 1965.
- [8] P. Silvester, "TEM properties of microstrip transmission lines," *Proc. Inst. Elec. Eng. (London)*, vol. 115, pp. 43-48, Jan. 1968.
- [9] T. C. Bryant and J. A. Weiss, "Parameters of microstrip transmission lines and coupled pairs of microstrip lines," *IEEE Trans. Microwave Theory Tech.*, vol. MTT-16, pp. 1021-1027, Dec. 1968.
- [10] E. Yamashita and K. Atsuki, "Analysis of thick transmission lines," *IEEE Trans. Microwave Theory Tech.*, vol. MTT-19, pp. 120-122, Jan. 1971.
- [11] E. Yamashita and R. Mittra, "Variational method for the analysis of microstrip lines," *IEEE Trans. Microwave Theory Tech.*, vol. MTT-16, pp. 251-256, Apr. 1968.
- [12] E. Yamashita, "Variational method for the analysis of microstrip-like transmission lines," *IEEE Trans. Microwave Theory Tech.*, vol. MTT-16, pp. 529-535, August 1968.
- [13] M. K. Krage and G. I. Haddad, "Characteristics of coupled microstrip transmission lines: I—Coupled mode formulation of inhomogeneous lines; II—Evaluation of coupled line parameters," *IEEE Trans. Microwave Theory Tech.*, vol. MTT-18, pp. 217-228, Apr. 1970.
- [14] H. G. Bergaudt and R. Pregla, "Calculation of even and odd mode capacitance parameters for coupled microstrips," *Arch. Elek. Übertragung*, vol. 26, pp. 153-158, Apr. 1972.
- [15] I. J. Bahl and P. Bhartia, "Characteristics of inhomogeneous-coupled stripline," *IEEE Trans. Microwave Theory Tech.*, vol. MTT-28, pp. 529-535, June 1980.
- [16] D. L. Gish and O. Graham, "Characteristic impedance and phase velocity of a dielectric-supported air-strip transmission line with side walls," *IEEE Trans. Microwave Theory Tech.*, vol. MTT-18, pp. 131-146, Mar. 1970.
- [17] E. Yamashita and K. Atsuki, "Stripline with outer conductor and three dielectric layers," *IEEE Trans. Microwave Theory Tech.*, vol. MTT-18, pp. 238-244, May 1970.
- [18] J. L. Allen and M. F. Estes, "Broadside-coupled strips in a layered dielectric medium," *IEEE Trans. Microwave Theory Tech.*, vol. MTT-20, pp. 662-669, Oct. 1972; also, correction, *IEEE Trans. Microwave Theory Tech.*, vol. MTT-23, p. 779, Sept. 1975.
- [19] S. K. Koul and B. Bhat, "Characteristic impedance of microstrip-like transmission lines for millimeter wave applications," *Arch. Elek. Übertragung*, vol. 35, pp. 253-258, June 1981.
- [20] S. K. Koul and B. Bhat, "Propagation parameters of coupled microstrip-like transmission lines for millimeter wave applications," in *IEEE MTT-S 1981 Int. Microwave Symp. Dig. (Los Angeles, CA)*, June 1981, pp. 489-491.

- [21] R. Crampagne, M. Ahmadpanah, and J. L. Guiraud, "A simple method for determining the Green's function for a large class of MIC lines having multilayered dielectric structures," *IEEE Trans. Microwave Theory Tech.*, vol. MTT-26, pp. 82-87, Feb. 1978.
- [22] R. E. Collin, *Field Theory of Guided Waves*. New York: McGraw-Hill 1960.

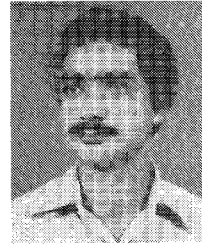


Bharathi Bhat received the B.E. degree in electrical communication engineering and the M.E. degree in electronics from the Indian Institute of Science, Bangalore, India, in 1963 and 1965, respectively. She continued her graduate studies at Harvard University, Cambridge, MA, and received the M.S. and Ph.D. degrees in applied physics in 1967 and 1971, respectively.

From 1971 to 1972 she worked as a Post-Doctoral Research Fellow in the Division of Engineering and Applied Physics, Harvard University. In 1973 she joined the Indian Institute of Technology (I.I.T.), New Delhi, India, as Assistant Professor. Since 1977 she has been a Professor and is currently the Head of the Centre for Applied Research in Electronics (CARE) at I.I.T., New Delhi. She is the leader of the Microwave Group in CARE and has been directing experimental research projects on microstrip and slotline components, monopulse antenna, and electronic phase shifters. Currently, she is also engaged in research and development

in the areas of printed antennas and millimeter wave circuits, specifically inverted microstrip, fin-line and insular image guide components.

Dr. Bhat is a Fellow of the Institution of Electronics and Telecommunication Engineers (IETE). She is presently the Honorary Editor of the IETE journal (Electromagnetics Section) and is also a member of the IETE Council.



Shiban K. Koul (S'81) received the B.E. degree in electrical engineering from Regional Engineering College, J & K, India, in 1977 and the M. Tech. degree in radar and communication engineering from the Indian Institute of Technology, Delhi, India, in 1979.

From 1979 to 1980 he worked as a senior research assistant in the Centre for Applied Research in Electronics (CARE) at I.I.T., New Delhi. Since 1980 he has been a Senior Scientific Officer and is working as a part time student towards the Ph.D. degree. Currently, he is engaged in research activities in the areas of thin-film microwave integrated circuits, electronically controlled ferrite phase shifters, and millimeter wave transmission lines.

Mr. Koul was awarded a gold medal by the Institution of Engineers, India, for securing first position among all the disciplines of engineering in the B.E. degree course.

A Review of SAW-Based Direct Frequency Synthesizers

ALAN J. BUDREAU, MEMBER, IEEE, ANDREW J. SLOBODNIK, MEMBER, IEEE, AND PAUL H. CARR, FELLOW, IEEE

Abstract—Many new electronic systems, including spread spectrum links, require frequency synthesizers capable of providing accurate signals of high spectral purity, and must be able to change frequencies in fractions of a microsecond. Three such synthesizers based on comb generators, SAW filterbanks, and fast switches are reviewed. Each of these synthesizers can provide an output at approximately 1.3 GHz from one of over 200 frequencies of integral megahertz value.

I. INTRODUCTION

SURFACE ACOUSTIC wave (SAW) components offer a compact cost-effective way to make a variety of components, including filters [1], delay lines [2], correlators

Manuscript received November 4, 1981. A condensed version of this paper has been presented at the 1981 IEEE-MTT International Microwave Symposium, Los Angeles, CA.

The authors are with the Electromagnetic Sciences Division, Rome Air Development Center, Hanscom AFB, MA 01731.

[3], and frequency synthesizers [4]–[6]. This last application is the subject of this paper. In particular, a review of recent work on the use of SAW devices for obtaining fast-frequency hopping, direct frequency synthesis will be provided.

Direct synthesis [7] is useful whenever submicrosecond frequency hopping is required in combination with high spectral purity and frequency precision that is as good as the reference clock. To these features, SAW's add their traditional advantages of small size and moderate cost. The basic version of the direct SAW frequency synthesizer [8], [9] consists of a comb generator and switchable filterbank as shown in Fig. 1. The comb spectrum is simultaneously fed to all channels of the filterbank which sorts them according to frequency. Since the tones present at the filter outputs are continuous waves (CW), they can be switched